



# Direct Speed Control Scheme for Maximum Power Point Tracking of a 1.5MW DFIG Wind Turbine

Edy Ayala<sup>1</sup> , Nicolás Pozo<sup>1</sup> , Silvio Simani<sup>2</sup> , and Eduardo Muñoz<sup>1</sup> 

<sup>1</sup> Universidad Politécnica Salesiana, Calle Vieja 12/30, Cuenca, Ecuador  
eayala@ups.edu.ec, {apozoa, emunozp2}@est.ups.edu.ec

<sup>2</sup> Ferrara University, Via Savonarola, 9, 44121 Ferrara, FE, Italy  
silvio.simani@unife.it

**Abstract.** In the present work, a control strategy for Maximum Power Point Tracking (MPPT) applied to a wind turbine is described. The electric machine consists of a 1.5MW Doubly Fed Induction Generator (DFIG). This strategy is developed according to the theory of Direct Speed Control (DSC), which includes a state observer. This strategy considers the Low Shaft Speed (LSS) as an input and the  $i_{qr}$  reference current as the output. This control mechanism allows monitoring the MPPT; thus, changing the Power Coefficient ( $C_p$ ) to its optimal value during the wind turbine operation. Among its main features, the controller is configured to work with the incorporation of different wind inputs, a fact that permits evaluating the system's response to disturbances and variations. For simulation tests, a wind turbine has been modeled in MATLAB-Simulink and Fatigue, Aerodynamics, Structures and Turbulence (FAST) software. The strategy has been compared to a PI-MPPT controller and has demonstrated improvements in terms of speed and output power extraction.

**Keywords:** Power coefficient · MPPT · Direct speed control · DFIG · Wind turbine

## 1 Introduction

The demand for wind power generation, added to the depletion of natural resources, has been the main generators of the environmental and energy crises. Consequently, both factors led to the search for renewable energy sources that would significantly contribute to energy production. It is estimated that the generation of wind energy will be 20% of the world's total electricity by 2040 [1]. Within the production of wind energy through renewable resources, wind energy has implied important changes in the generation and control systems of wind turbines. In the case of control systems, they are very important in the operation of a wind turbine system [2, 3]. Currently, the wind turbine market is aimed at high power generation systems (from 1 MW), and for these applications,

DFIGs are of great interest since they are capable of extracting high power thanks to their low-cost power converters and low energy losses in comparison to other types of devices [4, 5].

The control strategy allows manipulating the slip angle between  $\pm 30\%$  of the synchronous speed of operation. For the maximum power point controller design, MPPT is implemented by considering the wind speed, the rotor speed, the power generated, and the angle of inclination of each blade as variables. The control strategy seeks to improve the maximum power curve response through a direct speed controller (DSC) and the LSS as input. The controller also implements a state observer, which allows estimating the response to a random input of wind [6]. The following article shows a DSC strategy to obtain the maximum power point using a state observer. For the simulation and validation of results, a 1.5 MW wind turbine was selected by using MATLAB-Simulink and FAST [7, 8].

For explanation purposes, section two presents the description of the system, and section three presents the analysis and modeling of the subsystems that directly intervene in the operation of the wind turbine as well as the description of the parameters that have been used for the DSC simulation. In detail, section four shows the control strategy and simulations based on FAST and Simulink. Finally, section five discusses the validation results.

## 2 System Description

A wind turbine is a device that transforms energy from the wind into electric power. The wind turbine is composed of the following systems: aerodynamic model, pitch angle control, mechanical, electrical, and control systems sized according to torque. In Fig. 1, the interaction between the different systems that make up the wind turbine is shown [6, 9].

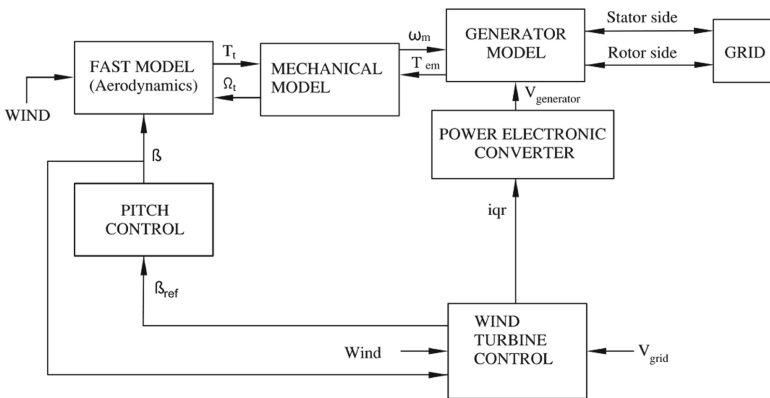


Fig. 1. Block diagram of the systems of a DFIG wind turbine.

### 2.1 Aerodynamic Model

The wind turbine blades convert the wind energy into rotational energy. Thereon, the extracted energy is represented by an aerodynamic model, which mainly represents the speed and torque as a function of the input wind. In terms of the wind speed, it can be considered as the average speed of the incident wind in the area swept by the blades in order to evaluate the torque at the low shaft speed. The output power of the wind turbine can be modeled in terms of the power coefficient, blade length, wind speed, and air density [10, 11]. These terms can be formulated by the relationships in the set of Eq. (1).

$$P_r = \frac{1}{2} \rho \pi R^2 W^3 C_p(\lambda, \beta); \quad T_r = \frac{1}{2} \rho \pi R^3 W^2 C_q(\lambda, \beta) \tag{1}$$

Where  $\rho$  is the air density,  $R$  is the blade length,  $W$  is the input wind speed,  $C_p$  is the power coefficient,  $\lambda$  is the tip speed ratio,  $\beta$  is the pitch angle, and  $C_q$  is the torque coefficient [10]. Betz’s law constitutes a maximum generation limit for a wind turbine, establishing the restriction of 59.26% of the wind energy to mechanical energy transfer. This limit is known as the power coefficient and is described as a complex relationship of the tip speed ratio and the blade pitch angle stated in [12]. For each  $\beta$  angle, it corresponds to an optimal tip speed ratio at which the power coefficient  $C_p$  is the maximum value [13]. Defined by Eq. (2),  $C_p$  is often given as a function of  $\lambda$ .

$$C_p = c1 \cdot \left[ \frac{c2}{\lambda_i} - c3 \cdot \beta - 5 \right] e^{\frac{-c4}{\lambda_i}} + c5 \cdot \lambda; \quad \lambda_i = \left[ \frac{1}{\lambda + c6 \cdot \beta} - \frac{c7}{(\beta^3 + 1)} \right]^{-1};$$

$$\lambda = \frac{R * \Omega_t}{W} \tag{2}$$

Where  $\Omega_t$  is the LSS, and  $c1$  to  $c6$  are constants usually given by the manufacturer or obtained experimentally.

### 2.2 Mechanical Model

The mechanical model consists of all moving components that allow the energy transference from the wind to the electric generator. It includes the drivetrain, blades, rotor hub, tower, nacelle, and rotating mechanisms. With reference to the drivetrain, it encompasses models depending on the number of masses for the dynamic analysis. For these experiments, a two-mass has been analyzed following the recommendations in [8] shown in Fig. 2. The drivetrain model establishes the relationships between the inertias, torques, angular speeds, damping, and friction factors described in Eq. (3).

$$J_t \frac{d\Omega_t}{dt} = T_t - D_t \Omega_t - T_{em}; \quad J_m \frac{d\Omega_m}{dt} = T_{em} - D_m \Omega_m + T_{em}$$

$$\frac{dT_{em}}{dt} = K_{tm}(\Omega_t - \Omega_m) + D_{tm} \left( \frac{d\Omega_t}{dt} - \frac{d\Omega_m}{dt} \right) \tag{3}$$

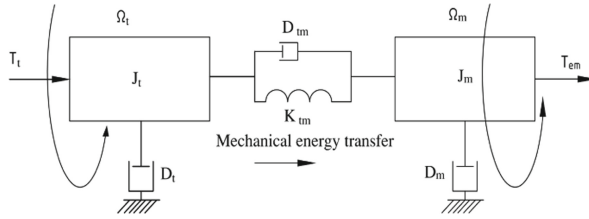


Fig. 2. Two-mass mechanical model.

Where,  $J_t$  is the turbine inertia,  $J_m$  is the machine inertia,  $\Omega_m$  is the High Shaft Speed (HSS), the damping coefficients of the turbine, machine, and drivetrain are ( $D_t$ ,  $D_m$ , and  $D_{tm}$ ) respectively, and the stiffness constant ( $K_{tm}$ ); thus, resulting in a two-inertia model [6, 12].

### 2.3 Pitch Control System

The main job of the controller is to rotate the wind turbine blades at different angles to increase or decrease the speed of the rotor. Currently, the controllers can even manipulate the inclination of each blade independently. This advantage gives greater versatility since having more combinations of positions can reduce the stress on the blades.

The rotation of the angle is controlled, as shown in Fig. 3, by a proportional integrative controller PI that generates a reference rate of speed change. The angle of inclination itself is obtained by integrating the variation of the angle [14].

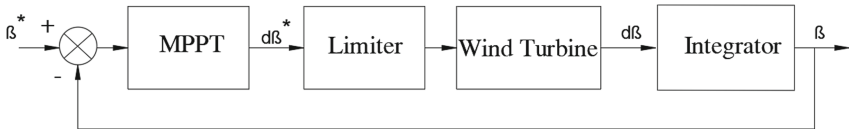


Fig. 3. Pitch angle control system.

The pitch controller is very important for a wind turbine because a mechanical control of the torque is needed in order to regulate the generator HSS, which leads the reference to maintain optimum operating speed. This response is slow, but it is necessary in order to guarantee the nominal speed operation of the system and regulate the wind turbine once it enters into a full operation zone. The idea is to reduce the speed before it is needed to apply the brake system, which produces high friction.

## 3 Direct Speed Control

Direct speed control has an advantage over other control methods in that it follows the power curve with a much faster response. By knowing  $\lambda$ , the estimated optimum wind turbine rotation speed  $\Omega_{m\_ref}$  can be calculated. For real scenarios, wind speed is not

a real variable because the turbine itself creates shadow effects that alter its measurements. The optimum rotational speed is better calculated from the torque. Therefore, it is possible to design an observer to calculate the torque by measuring variables such as the electromagnetic torque  $T_{em}$  and the HSS, which are used for estimating the optimal speed  $\Omega_{m\_ref}$  (4) [15].

$$\Omega_{m\_ref} = N \sqrt{\frac{T_{t\_est}}{k_{opt\_t}}} \tag{4}$$

Where  $N$  is the drivetrain ratio,  $T_{t\_est}$  is the aerodynamic estimated torque, and  $k_{opt\_t}$  is the optimum constant for MPPT observer that allows adjusting  $\Omega_{m\_ref}$  by using the  $T_{em}$ . The DSC general scheme presented in [6] for these experiments is shown in Fig. 4.

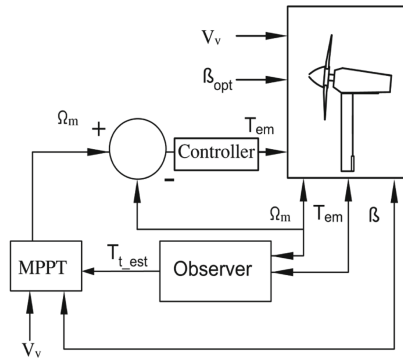


Fig. 4. Direct speed control block diagram.

In this article, the observer is implemented for a MPPT controller. When the  $C_p$  is at its maximum value, the low shaft torque  $T_{t\_est}$  can be calculated as described in Eq. (5).

$$T_{t\_est} = \frac{1}{2} \rho \pi \frac{R^5}{\lambda_{opt}^3} C_{p\_max} \Omega_t^2 = k_{opt} \Omega_t^2 \tag{5}$$

Finally, the above equation allows having a relationship in terms of  $k_{opt\_t}$  described in Eq. (6).

$$k_{opt\_t} = \frac{1}{2} \rho \pi \frac{R^5}{\lambda_{opt}^3} C_{p\_max} \tag{6}$$

All the above equations have been simulated in MATLAB-Simulink, and for the aeroelastic wind model, the software FAST has been used for modeling a wind turbine as a combination of mechanical elements and their interactions. For this article, a three blades turbine has been modeled as a combination of rigid and flexible elements [8, 14].

### 3.1 DSC Control Description

The controller presented in Fig. 4 considers the angular velocity of the rotor as input, and together with expression (5), the  $T_{t\_est}$  is calculated. This low shaft torque, by means of a state observer block, allows generating the estimated electromagnetic torque control signal to regulate the wind turbine output power [7, 14].

The dynamic system has internal conditions at determined points that are monitored by the state observer based on the Luenberger algorithm. In order to establish the control strategy, the observer may have a complete or reduced order depending on the monitored states. Once the estimated state data are computed, the signal error is calculated by the gain of the estimator, which depends on the system. For these experiments, the gain is unitary, as shown in Fig. 5, and in Fig. 6, the implementation of the controller in MATLAB-Simulink is illustrated. For the calculation of the current  $i_{qr}$  which enters the PI control block, the following expression (7) is used and calculated from the generated electromagnetic torque [16].

$$T_{em} = -\frac{3}{2}p \frac{L_m}{L_s} \Psi_s i_{qr} \tag{7}$$

Where  $p$  is the wind turbine pairs of poles;  $\Psi_s$  is the stator flux frame;  $L_m$  is the mutual inductance, and  $L_s$  is the stator inductance.

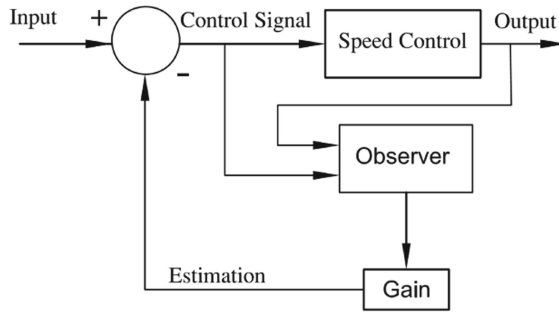


Fig. 5. Feedback of observed states block diagram.

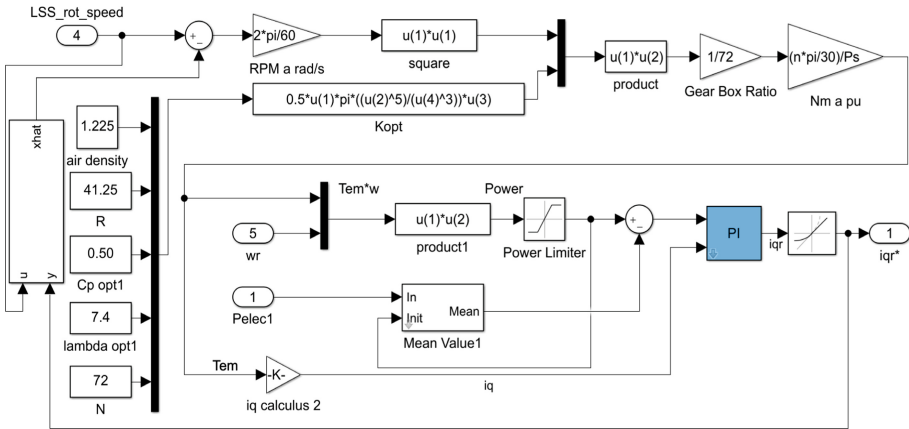


Fig. 6. Direct speed controller implementation in MATLAB-Simulink

### 4 Simulation Results

In this section, the dynamic response of the DSC state observer is detailed. For this work, three types of wind inputs are used in order to validate the obtained results. In all cases, the wind turbine rapidly and accurately reaches the optimal operating point by using the DSC state observer.

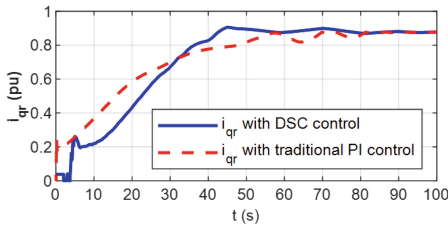
The following outputs are considered in order to evaluate the system’s dynamic response: reference signal  $i_{qr}$  in p.u, the electromagnetic torque in Nm, the active output power in Watts, the wind input in m/s, the generator speed in rpm, the pitch angle in degrees, and the power coefficient.

#### 4.1 Steady Wind Speeds with Ramp Type Transitions

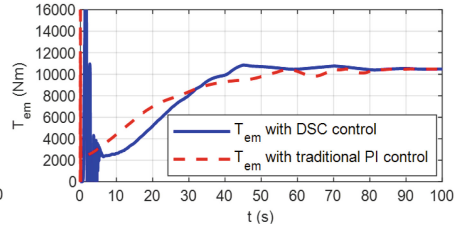
It can be seen the results of the system behavior in Fig. 7. The DSC Luenberger state observer tracks the  $C_p$  value with a more rapid response. The  $C_p$  dynamics, in this case, is improved compared with the PI controller Fig. 7(g). The produced output power using this DSC strategy in comparison with the classical PI controller is also more stable Fig. 7(b).

#### 4.2 Variable Wind Speed with Realistic Input

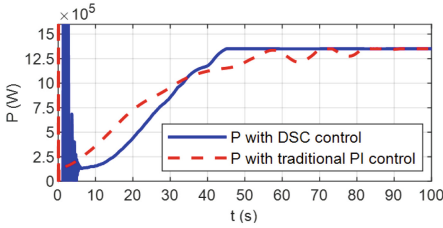
A realistic wind speed was used in this test to demonstrate the dynamic response. The results can be observed in Fig. 8. The DSC state observer tracks the  $C_p$  value with more quick dynamics. The  $C_p$  response, in this case, is better than the PI controller Fig. 8(g). The MPPT rapidly responds to wind changes; thus, achieving a better response in the optimal operating parameters.



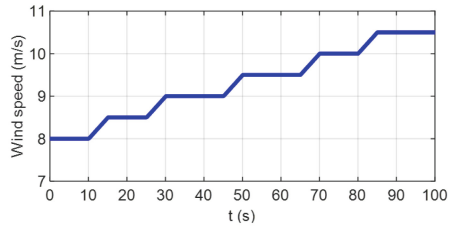
(a)



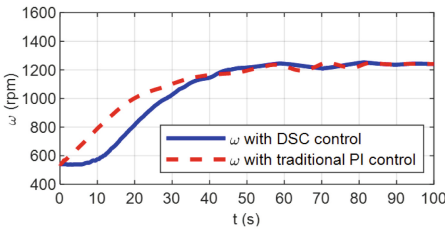
(b)



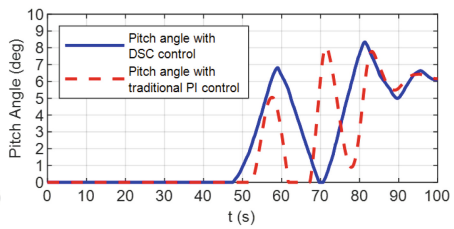
(c)



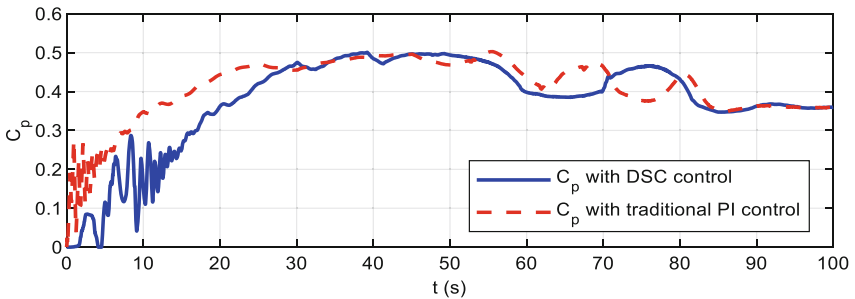
(d)



(e)



(f)



(g)

**Fig. 7.** Steady wind speed with ramp type transitions: reference signal  $i_{qr}$  in p.u. (a), electromagnetic torque in Nm (b), output power in W (c), wind speed in m/s (d), HSS in rpm (e),  $\beta$  in degrees (f) and  $C_p$  (g).



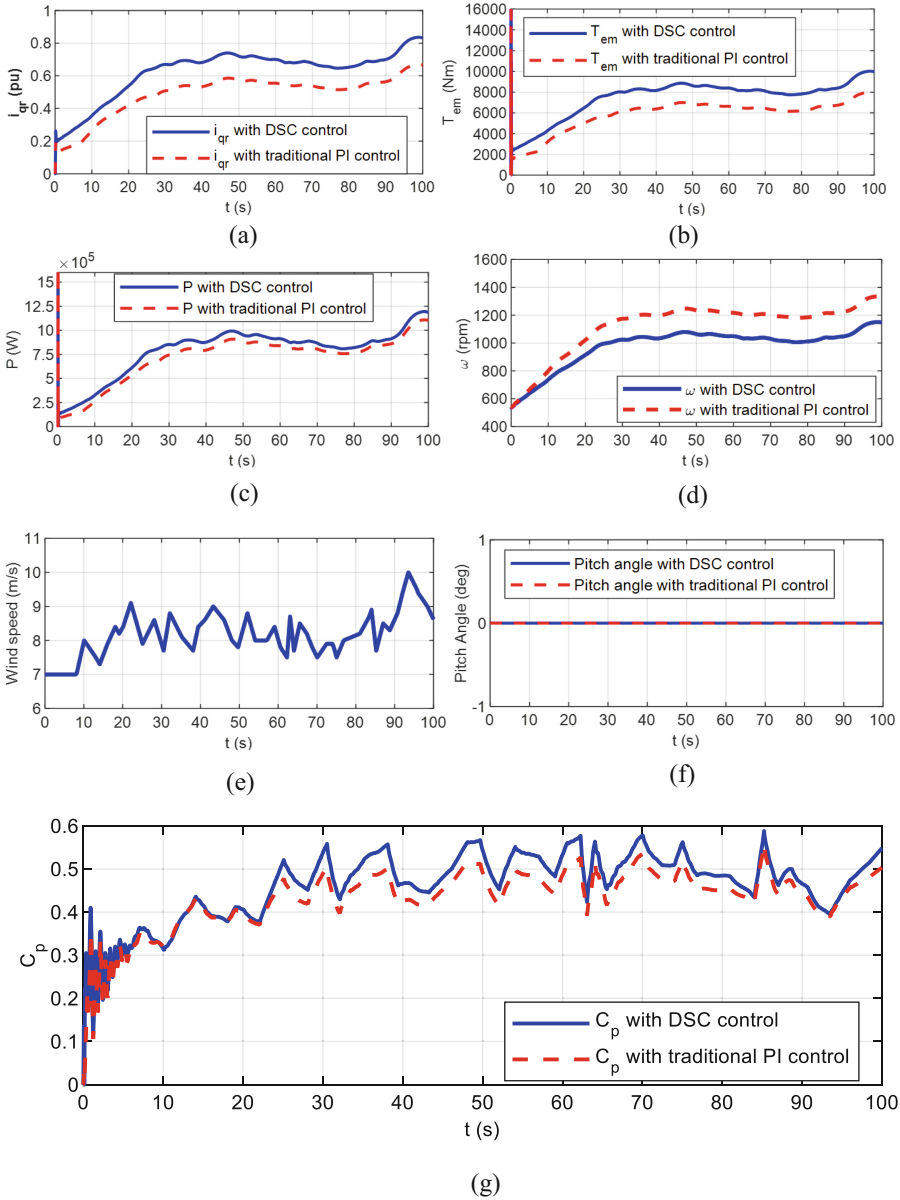


**Fig. 8.** Realistic wind speed input: reference signal  $i_{qr}$  in p.u. (a), electromagnetic torque in Nm (b), output power in W (c), wind speed in rpm (d), HSS in rpm (e),  $\beta$  in degrees (f) and  $C_p$  (g).

## 5 Conclusions

It is worth noting that, for any wind turbine, the MPPT is an important strategy that allows more power extraction. An appropriate model and control design are key factors not only in terms of operation but also in terms of maintenance and durability of the elements. Although the wind speed is not always constant, MPPT can still track the dynamic response of the system, a feat that makes it an interesting strategy. When a proper MPPT is performed, a more reliable energy system can be guaranteed, and by adding contributions of individual generators into wind farms, the influence of the controller becomes evident.

The DSC strategy based on the Luenberger state observer has allowed the system to operate with a better power extraction and  $C_p$ . Although the system is unstable during the first seconds of simulation due to the initial conditions, it rapidly reaches the optimum values. This means more active power available and absorption of reactive power from the grid. The advantage of this technique is also that the observer does not require any additional hardware implementation since it requires only the wind turbine system available measurements. For further implementations, it can even increase the number of input parameters for improving the accuracy.

In addition, this observer allows a close route of the feedback signals in order to minimize the error close to zero. The observer easily tracks the convex  $C_p$  function. The complementary DSC strategy allows the wind turbine to produce more torque and power by progressive variations of  $i_{qr}$ . The HSS is not increased in order to maximize the output power; instead, it is reduced in comparison to the classical-PI. This means that the mechanical components are slightly reduced in terms of fatigue, and the operative lifetime of the mechanical components can be improved. Finally, this controller is modular and can be implemented over an operative wind turbine.

Finally, this work includes simulations using data from manufacturers and published papers. However, the present research should include real implementations using hardware in the loop strategies in order to test the proposed scheme with a real DFIG. Moreover, it will be necessary to include real wind speed profiles in order to analyze a more accurate dynamic response. Additionally, other experiments can be performed, including other electric machine technologies such as PMSG in order to demonstrate the versatility of the proposed method.

## References

1. World Wind Energy Association (2010) World Wind Energy Report 2010. WWEA
2. Zhi-Nong W (2009) The intelligent control of DFIG-based wind generation. In: Conference on sustain power generation and Supply, pp 1–5
3. Ayala E, Simani S (2019) Perturb and observe maximum power point tracking algorithm for permanent magnet synchronous generator wind turbine systems. In: Proceedings of the 15th European workshop on advanced control and diagnostics, pp 1–11
4. Muller S, Deicke M, Doncker R (2000) Doubly-fed induction generators systems for wind turbines. IEEE Indu Appl Mag 8(3):26–33
5. Sow TL (2012) Nonlinear control of the wind turbine at DFIG for a participation to the regulating of the frequency of the network, Quebec

6. Abad G, Lopez J, Rodriguez M, Marroyo L, Iwanski G (2011) Doubly fed induction machine. Wiley
7. The MathWorks Inc. MATLAB-Simulink, Massachusetts
8. National Renewable Energy Laboratory (2020) Fatigue aerodynamics structures and turbulence
9. Tremblay E, Atayde S, Chandra A (2009) Direct power control of a DFIG-based WECS with active filter capabilities. In: IEEE electrical power energy
10. Magdi M, Mojeed O (2019) Adaptive and predictive control strategies for wind turbine systems: a survey. *IEEE J Autom SINICA* 6:364–378
11. Hallak M, Hasni M, Mena M (2018) Modeling and control of a doubly fed induction generator base wind turbine system. In: 3rd CISTEM 2018
12. Gajewski P, Pienkowski K (2016) Direct torque control and direct power control of wind turbine system with PMSG. Wrocław University of Technology, Department of Electrical Machines, Drives and Measurements
13. Mendis N, Muttaqi K, Sayeef S, Perera S (2012) Standalone operation of wind turbine-based variable speed generators with maximum power extraction capability. *IEEE Trans Energy Convers* 27(4):822–834
14. NREL (2014) Simulation for wind turbine generators—with FAST and MATLAB-simulink modules, USA
15. Camblong H (2006) Experimental evaluation of wind turbines maximum power point tracking controllers. *Energy Convers Manage* 47(11):2846–2858
16. Mohammadi J, Vaez-Zadeh S, Afsharnia S, Daryabeigi E (2014) A combined vector and direct power control for DFIG-based wind turbines. *IEEE Trans Sustain Energy* 5(3):767–775